JACS
JOURNAL OF THE AMERICAN CHEMICAL SOCIETY
pubs.acs.org/JACS
Communication

Room-Temperature Synthesis of Zeolite Membranes toward Optimized Microstructure and Enhanced Butane Isomer Separation Performance

Yi Liu, Sixing Chen, Taotao Ji, Jiahui Yan, Kaishi Ding, Shengyan Meng, Jinming Lu, and Yi Liu*

Cite This: J. Am. Chem. Soc. 2023, 145, 7718–7723
Read Online
ACCESS | Metrics & More | Article Recommendations | Supporting Information

ABSTRACT: Room temperature (RT) synthesis of high-performance zeolite membranes, which is profound from techno-economic and eco-friendly perspectives, remains a grand challenge. In this work, we pioneered the RT preparation of well-intergrown pure-silica MFI zeolite (Si-MFI) membranes, which was realized through adopting highly reactive NH_4F-mediated gel as nutrient during epitaxial growth. Benefiting from the introduction of fluoride anions as mineralizing agent as well as precisely tuned nucleation and growth kinetics at RT, both their grain boundary structure and thickness could be deliberately controlled, resulting in the formation of Si-MFI membranes showing unprecedented *n*-/*i*-butane separation factor (96.7) and *n*-butane permeance (5.16×10^{-7} mol m^{-2} s^{-1} Pa^{-1}) in the case of a feed molar ratio of 10/90, which well transcended the state-of-the-art membranes reported in the literature. This RT synthetic protocol was also proven effective for preparing highly *b*-oriented Si-MFI film, thus showing great promise for the preparation of diverse zeolite membranes with optimized microstructure and superior performance.

Zeolite membranes have received extensive attention for energy efficient separation, owing to their well-defined pore structure, robust framework, and excellent stability.[1−5] Previous studies confirmed that the microstructure of zeolite membranes, including preferred orientation, membrane thickness, and grain boundary structure, exerted significant influence on their separation performance.[6,7] For instance, the superior performance of *b*-oriented MFI zeolite membranes has been demonstrated for isomer separation (e.g., *n*-/*i*-butane and *p*-/*o*-xylene),[8−10] while defect-free ultrathin zeolite membranes commonly exhibited superior gas separation performance.[11,12] It should be noted that, in spite of significant progress on microstructure optimization and performance enhancement of zeolite membranes, under most circumstances, zeolite membrane growth has to be performed at relatively high temperature (commonly >100 °C), which inevitably leads to increased capital investment, operating cost, and energy consumption; simultaneously, safety concerns have to be taken into consideration under autogenous pressure.[13−15]

Recently, significant efforts have been devoted to reducing the reaction temperature of zeolite membranes. Diverse approaches, e.g., reactive growth,[13] flux synthesis,[16] and microwave heating[14,17,18] have been developed for mild synthesis of zeolite membranes. However, room temperature (RT) synthesis of continuous zeolite membranes, which is advantageous in terms of economic and environmental benefits, remains a great challenge. For instance, external energy input is considered indispensable for preparing continuous MFI zeolite membranes,[13] owing to the difficulty in overcoming the energy barrier between TPA-silicalite precursors and MFI zeolite crystallites at RT.

Previous studies revealed that incorporating fluoride anions in precursor solution was beneficial for the formation of zeolite membranes with fewer lattice and grain boundary defects, relying on the variation of electron density around silicon precursors through the formation of $[SiO_{4/2}F]^-$ intermediates, which fulfilled the charge balance for template cations instead of internal silanol defects;[19−21] in addition, the mineralizing effect reinforced by fluoride-containing species has proven to be effective for accelerating the crystallization rate of zeolites,[19,22,23] making it possible for RT synthesis of MFI zeolite membranes with optimized microstructure and enhanced performance.

Motivated by the above considerations, in this study, we pioneered RT synthesis of pure-silica MFI zeolite (Si-MFI) membranes (Figure 1): Initially, a procedure combining preliminary aging with fluoride-assisted crystallization was employed for preparing a semisolid gel. Subsequently, spin-coating was employed for depositing the Si-MFI seed layer on porous α-Al_2O_3 substrate. In the next step, RT epitaxial growth was conducted relying on the above gel, resulting in the formation of a well-intergrown Si-MFI membrane with superior *n*-/*i*-butane separation performance. Following the same synthetic protocol, twin-free and highly *b*-oriented Si-MFI film was further prepared, thus showing great promise for RT synthesis of diverse zeolite membranes with optimized microstructure and superior performance.

The first step involved the preparation of Si-MFI seeds. The SEM image indicated that uniform Si-MFI seeds with an

Received: January 1, 2023
Published: March 3, 2023

https://doi.org/10.1021/jacs.3c00009
J. Am. Chem. Soc. 2023, 145, 7718−7723

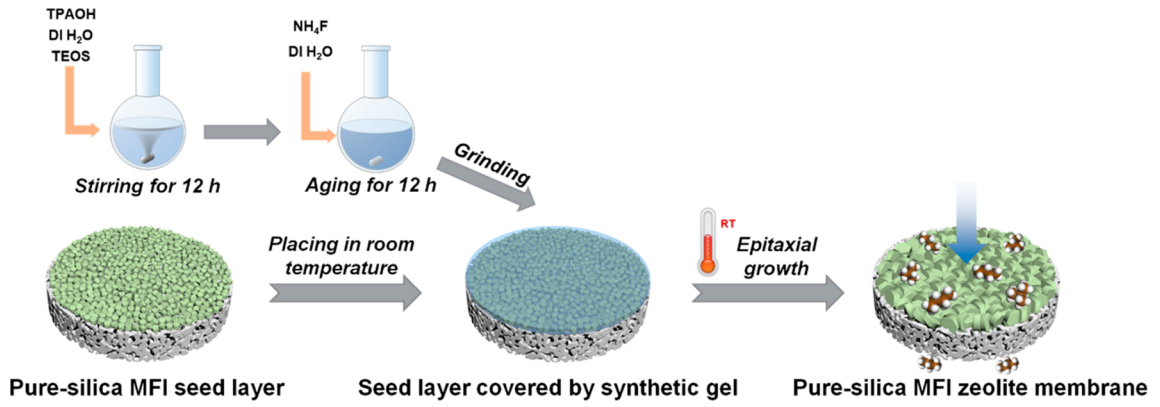

Figure 1. Schematic illustration of the Si-MFI membrane fabrication process via RT epitaxial growth.

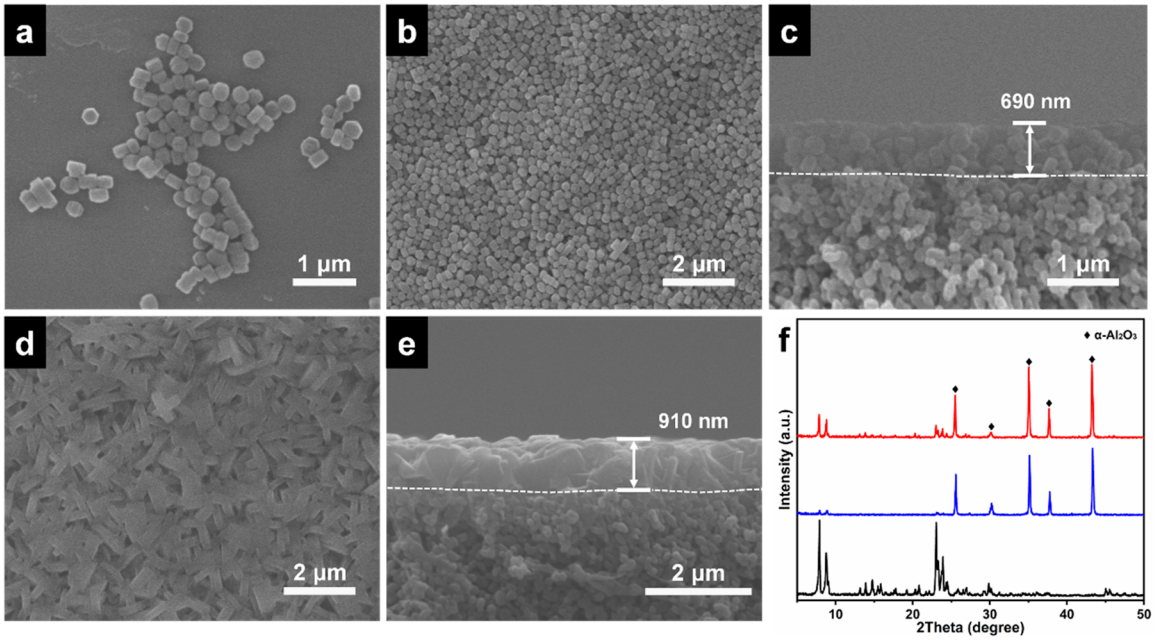

Figure 2. SEM images of (a) Si-MFI seeds. Top and cross-sectional SEM images of the (b, c) prepared Si-MFI seed layer and (d, e) Si-MFI membrane after RT epitaxial growth; (f) XRD patterns of Si-MFI seeds (black line), the Si-MFI seed layer (blue line), and the synthesized Si-MFI membrane (red line).

average size of 240 nm could be obtained via a facile hydrothermal route (Figure 2a). After spin-coating under optimized conditions, a uniform and closely packed 690 nm-thick Si-MFI seed layer was deposited on the porous α-Al_2O_3 substrate (Figure 2b,c). Subsequently, RT epitaxial growth was carried out to seal intergranular gaps in the seed layer, during which a fluoride-containing semisolid gel served as the nutrient source. SEM images indicated that prolonging the reaction duration led to gradual sealing of intercrystalline defects (Figure S1). After reaction for 12 weeks, a well-intergrown Si-MFI membrane with a thickness of 910 nm and grain size of 850 nm was readily formed (Figure 2d,e). To the best of our knowledge, this represented the lowest reaction temperature ever reported regarding zeolite membrane preparation. The corresponding XRD pattern implied that the obtained membrane indeed belonged to the pure MFI phase (Figures 2f and S2).

It should be noted that the addition of NH_4F to the initial precursor played a crucial role in the formation of the well-intergrown Si-MFI membrane. As a comparative experiment, RT epitaxial growth was further conducted in the absence of NH_4F while keeping other conditions unchanged. Our results indicated that, after epitaxial growth for 12 weeks, the prepared Si-MFI membrane remained poorly intergrown (Figure S3). To better elucidate the growth mechanism of Si-MFI membranes, the initial precursors formed in the absence and presence of NH_4F were characterized. It was observed that a clear and colorless colloidal solution was formed before adding NH_4F (Figure S4a). The SEM image (Figure S5) indicated that the product was in amorphous bulk gel state and no evident particles with regular shapes were formed under this condition. After the addition of NH_4F, the clear colloidal solution was immediately solidified, accompanied with formation of white semisolid gels in the above solution (Figure S4b); moreover, the initial precursor structure changed dramatically. To be specific, the bulk colloidal aggregates disintegrated and oval-shaped 10−20 nm particles appeared instead (Figure S6). The variation in morphology could be attributed to the excellent mineralizing ability of fluoride anions, which not only changed the solubility of silica species

https://doi.org/10.1021/jacs.3c00009
J. Am. Chem. Soc. 2023, 145, 7718−7723

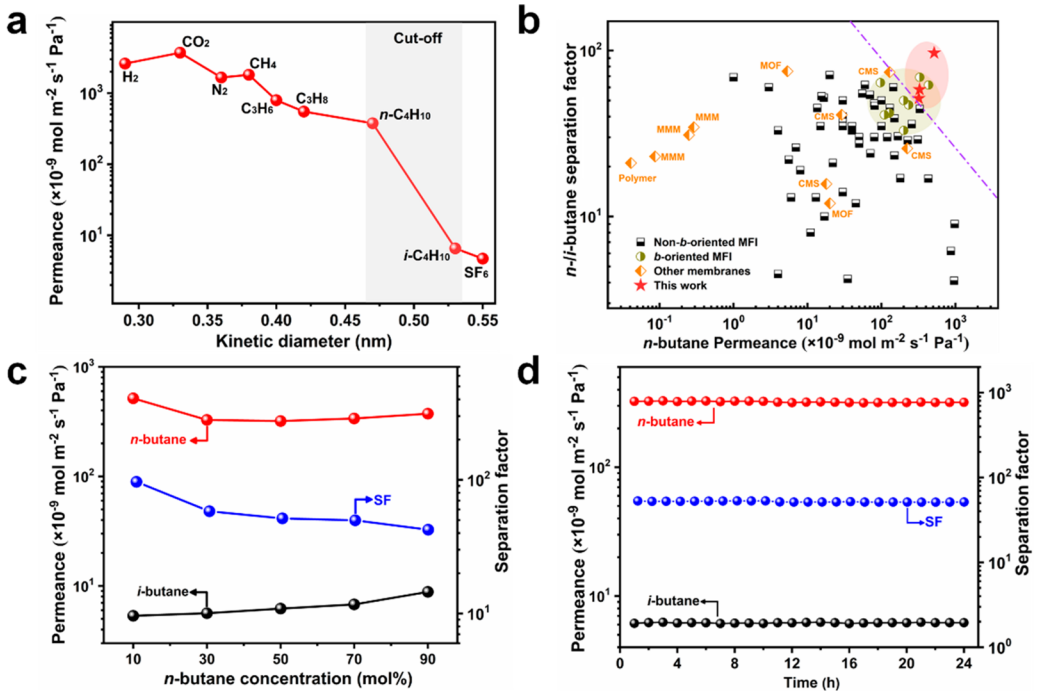

Figure 3. (a) Single-gas permeances of prepared Si-MFI membrane measured at 25 °C and 1 bar as a function of the molecular kinetic diameters. (b) Detailed comparison of *n*-/*i*-butane separation performance of prepared Si-MFI membranes with different *n*-butane feed concentrations (the concentration value from the left bottom to the right top corresponds to 50, 30, and 10, respectively) in this work with previously reported MFI zeolite membranes and other types of membranes. Detailed performance data are listed in Tables S2 and S3. The binary *n*-/*i*-butane separation performance of prepared Si-MFI membrane as a function of (c) *n*-butane feed concentration and (d) long-term stability of the prepared Si-MFI membrane for *n*-/*i*-butane separation.

but also reorganized their structure.[24] Regarding zeolite synthesis, it has been proposed that fluoride anions could serve as mineralizing agent to enhance the reactivity of silica species and, therefore, the crystallization rate.[23] Hence, it is reasonable to assume that the addition of NH_4F in initial precursor endowed epitaxial growth with higher crystallization rates, ultimately leading to the RT formation of continuous Si-MFI membrane.

To better elucidate the morphology evolution of zeolite membranes, the morphology and textural properties of sedimented gels before and after epitaxial growth were studied. According to XRD patterns, the NH_4F-containing gel was amorphous prior to epitaxial growth, and the first trace of MFI zeolite phase could be detected after 8 weeks (Figure S7). Further prolonging the reaction duration to 12 weeks led to a slight increase of the diffraction peak intensity of the MFI phase with precipitates remaining in a largely amorphous state (Figure S7). As further confirmed by SEM and TEM images, the precipitates were mainly composed of 10−20 nm-sized amorphous primary particles, which resembled those in the initial precursor; simultaneously, trace amounts of plate-like Si-MFI crystals were also observed (Figure S8). Results from N_2 adsorption/desorption isotherms further revealed that sedimented gels after RT epitaxial growth for different durations exhibited similar textural properties as those of the initial precursor (Figure S9 and Table S1), implying that initial gel was more inclined to serve as nutrients rather than initiate nucleation in the bulk solution during epitaxial growth. Through combining with a lower epitaxial growth rate at RT, more precise control over epitaxial growth kinetics could be achieved, resulting in the formation of the Si-MFI membrane with better intergrowth and controlled thickness, which was quite beneficial for improving the *n*-/*i*-C_4H_{10} (*n*-/*i*-butane) selectivity with no compromise in *n*-butane permeance.

Finally, gas permeation properties of the prepared Si-MFI membrane were evaluated in Wicke-Kallenbach equipment (Figure S10). Single gas permeation results demonstrated that the order of gas permeance through the membrane basically followed the same sequence as kinetic diameters of gas molecules; moreover, there existed a sharp permeance cutoff between *n*-butane (3.77×10^{-7} mol m^{-2} s^{-1} Pa^{-1}) and *i*-butane (6.54×10^{-9} mol m^{-2} s^{-1} Pa^{-1}). Of particular note, the ideal *n*-/*i*-butane selectivity reached 57.6, which was indicative of the existence of rare grain boundary defects in the membrane (Figure 3a). As for the equimolar *n*-/*i*-butane gas mixture, an *n*-butane permeance of 3.2×10^{-7} mol m^{-2} s^{-1} Pa^{-1} and separation factor (SF) of 51.5 were achieved under ambient conditions. In comparison with previous literature, the *n*-/*i*-butane separation performance of our membrane not only easily surpassed the upper bound limits for diverse types of membranes but also was superior to most MFI zeolite membranes reported in the literature (Figure 3b, Tables S2 and S3), which could be interpreted as follows: (1) The fluoride route endowed the membrane with reduced defects in the frameworks. (2) The RT epitaxial growth warranted well-controlled membrane thickness, morphology uniformity, and reduced grain boundary defects.

Simultaneously, the effect of feed composition on the *n*-/*i*-butane separation performance was investigated. As shown in Figure 3c, the SF of the *n*-/*i*-butane binary mixture was found to be positively associated with the *i*-butane feed composition, possibly owing to the crowding-out effect exerted by increased *i*-butane coverage, which amplified the molecular sieving

https://doi.org/10.1021/jacs.3c00009
J. Am. Chem. Soc. 2023, 145, 7718−7723

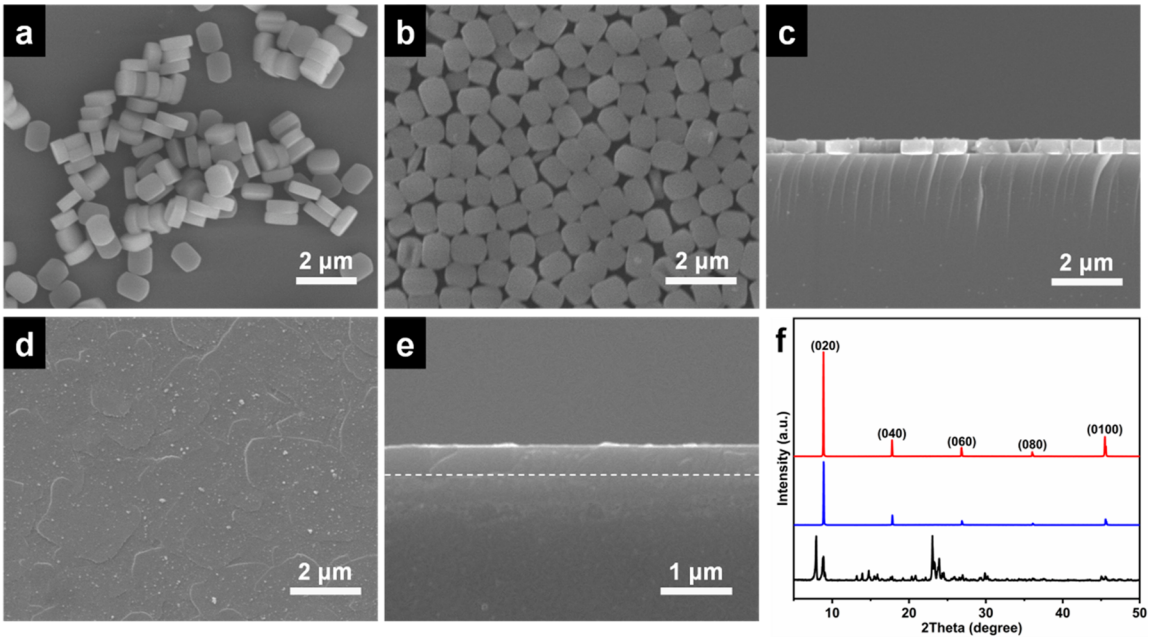

Figure 4. SEM images of (a) Si-MFI microcrystals. Top and cross-sectional SEM images of (b, c) the prepared Si-MFI seed layer and (d, e) Si-MFI film after RT epitaxial growth; (f) XRD patterns of Si-MFI microcrystals (black line), the Si-MFI seed layer (blue line), and the obtained Si-MFI film (red line).

effect.[25] Of particular note, a *n*-/*i*-butane SF of 96.7 and *n*-butane permeance of 5.16×10^{-7} mol m^{-2} s^{-1} Pa^{-1} could be obtained in the case of a feed molar ratio of 10/90, which ranked the highest among all separation membranes ever reported in the literature. In addition, pressure dependence of the separation performance of equimolar *n*-/*i*-butane mixture was studied (Figure S11a). Consistent with previous reports,[26−29] both the *n*-butane permeance and *n*-/*i*-butane SF decreased with increasing feed pressure, which could be attributed to the preferential intrusion of bulky *i*-butane that hindered the permeation of linear *n*-butane through zeolite pores.[28,30] With an increase in the feed pressure, the *n*-butane flux gradually increased, and the membrane exhibited a *n*-butane flux of 50.4 mmol m^{-2} s^{-1} upon increasing the feed pressure to 2.25 bar (Figure S11b). Aiming at practical application in industry, long-term stability of Si-MFI membranes was investigated (Figure 3d). Our results revealed that, after continuous operation over 24 h, both the *n*-butane permeance and *n*-/*i*-butane SF remained unchanged, which was indicative of excellent operation stability.

Preferred orientation control has proven to be essential for performance enhancement of zeolite membranes due to the ordered arrangement of pore aperture, reduced diffusion path length, and low grain boundary defect density. Previous studies indicated that inhibiting zeolite nucleation in the bulk solution was the key to twin suppression.[31−35] As mentioned above, the generation of highly reactive semisolid gel in bulk solution during RT epitaxial growth warranted not only a sufficient supply of nutrients for lateral epitaxial growth but also effective inhibition of bulk nucleation for twin growth, thus favoring the preparation of twin-free and highly *b*-oriented Si-MFI film.

To verify this deduction, we further conducted RT epitaxial growth from the *b*-oriented Si-MFI seed layer. Initially, a highly *b*-oriented 380 nm-thick seed layer was prepared by manual rubbing (Figure 4a−c).[14] Subsequently, RT epitaxial growth was carried out to seal the open space remaining in the seed layer. SEM results indicated that intercrystalline defects steadily decreased with prolonging the reaction duration (Figure S12). After 8 weeks, twin-free and well-intergrown Si-MFI film with smooth surface morphology was readily obtained (Figure 4d). The cross-sectional SEM image (Figure 4e) indicated that the film thickness reached 410 nm, which was only 8% higher than the thickness of the seed layer. In addition, an independent experiment tracking the growth process of Si-MFI seeds showed that the relative growth rates along the *a*, *b*, and *c* axes were *a*:*b*:*c* = 10:1:16, which unambiguously demonstrated the preferred lateral growth (*a*-, *c*-axis) of Si-MFI seeds during RT epitaxial growth (Figure S13 and Table S4). The XRD pattern (Figure 4f) showed only (0*k*0) characteristic peaks, which unambiguously confirmed the dominance of the preferred *b*-orientation. In addition, the precipitates sedimented at the bottom of the vessel after epitaxial growth remained dominantly amorphous (Figure S14). It is therefore reasonable to deduce that bulk nucleation rarely occurred during this process. To the best of our knowledge, this represented the lowest reaction temperature ever reported for the preparation of oriented zeolite films. Moreover, effects of the reaction temperature and synthetic gel composition on the morphology of Si-MFI films were further investigated. As shown in Figures S15 and S16, the duration for achieving continuous *b*-oriented Si-MFI films could be dramatically shortened upon increasing the synthesis temperature from RT to 80 °C. Meanwhile, it was found that there was no significant morphological difference between Si-MFI films obtained with different TPAOH concentrations (Figure S17). In addition, the effect of the NH_4F concentration on the quality of Si-MFI films was investigated (Figure S18). Obviously, the higher NH_4F concentration led to a shorter duration being required for the complete sealing of intergranular gaps in the seed layer.

To sum up, in this study, the RT synthetic protocol was developed for preparing high-quality Si-MFI membranes through employing a highly reactive NH_4F-mediated gel during epitaxial growth. The introduction of fluoride anions

https://doi.org/10.1021/jacs.3c00009
J. Am. Chem. Soc. 2023, 145, 7718−7723

as mineralizer and the conduction of the reaction at RT warranted an optimized structure at multiscale levels. Prepared Si-MFI membranes exhibited an *n*-/*i*-butane SF of 96.7 with *n*-butane permeance of 5.16×10^{-7} mol m^{-2} s^{-1} Pa^{-1} in the case of a feed molar ratio of 10/90, which ranked the highest among all separation membranes ever reported in the literature. Furthermore, well-intergrown and highly *b*-oriented Si-MFI films with few twins could be obtained at RT following the same procedure as above. We believe that a RT synthetic protocol could bring new insights into the facile preparation of diverse molecular sieve membranes with optimized microstructure and superior performance.

■ ASSOCIATED CONTENT

Supporting Information

The Supporting Information is available free of charge at https://pubs.acs.org/doi/10.1021/jacs.3c00009.

Detailed experimental procedures and instrument used; detailed characterization data of the synthetic gels for room temperature epitaxial growth and the obtained Si-MFI membranes/films; detailed gas separation performances of Si-MFI membranes (PDF)

■ AUTHOR INFORMATION

Corresponding Author

Yi Liu − *State Key Laboratory of Fine Chemicals, Frontiers Science Center for Smart Materials, School of Chemical Engineering and Dalian Key Laboratory of Membrane Materials and Membrane Processes, Dalian University of Technology, Dalian 116024, China;* orcid.org/0000-0002-2073-4832; Email: diligenliu@dlut.edu.cn

Authors

Yi Liu − *State Key Laboratory of Fine Chemicals, Frontiers Science Center for Smart Materials, School of Chemical Engineering, Dalian University of Technology, Dalian 116024, China*

Sixing Chen − *State Key Laboratory of Fine Chemicals, Frontiers Science Center for Smart Materials, School of Chemical Engineering, Dalian University of Technology, Dalian 116024, China*

Taotao Ji − *State Key Laboratory of Fine Chemicals, Frontiers Science Center for Smart Materials, School of Chemical Engineering, Dalian University of Technology, Dalian 116024, China*

Jiahui Yan − *State Key Laboratory of Fine Chemicals, Frontiers Science Center for Smart Materials, School of Chemical Engineering, Dalian University of Technology, Dalian 116024, China*

Kaishi Ding − *State Key Laboratory of Fine Chemicals, Frontiers Science Center for Smart Materials, School of Chemical Engineering, Dalian University of Technology, Dalian 116024, China*

Shengyan Meng − *State Key Laboratory of Fine Chemicals, Frontiers Science Center for Smart Materials, School of Chemical Engineering, Dalian University of Technology, Dalian 116024, China*

Jinming Lu − *State Key Laboratory of Fine Chemicals, Frontiers Science Center for Smart Materials, School of Chemical Engineering, Dalian University of Technology, Dalian 116024, China*

Complete contact information is available at: https://pubs.acs.org/10.1021/jacs.3c00009

Notes

The authors declare no competing financial interest.

■ ACKNOWLEDGMENTS

The authors are grateful to the National Natural Science Foundation of China (22205030, 22078039), Postdoctoral Science Foundation of China (2022M710579, 2022TQ0051), National Key Research and Development Program of China (2019YFE0119200), Fok Ying-Tong Education Foundation of China (171063), Science and Technology Innovation Fund of Dalian (2020JJ26GX026), Science Fund for Creative Research Groups of the National Natural Science Foundation of China (22021005), and the Fundamental Research Fundamental Funds for the Central Universities (DUT22LAB602) for the financial support.

■ REFERENCES

(1) Gascon, J.; Kapteijn, F.; Zornoza, B.; Sebastián, V.; Casado, C.; Coronas, J. Practical Approach to Zeolitic Membranes and Coatings: State of the Art, Opportunities, Barriers, and Future Perspectives. *Chem. Mater.* **2012**, *24*, 2829−2844.

(2) Algieri, C.; Drioli, E. Zeolite membranes: synthesis and applications. *Sep. Purif. Technol.* **2021**, *278*, 119295.

(3) Du, P.; Zhang, Y.; Wang, X.; Canossa, S.; Hong, Z.; Nenert, G.; Jin, W.; Gu, X. Control of zeolite framework flexibility for ultra-selective carbon dioxide separation. *Nat. Commun.* **2022**, *13*, 1427.

(4) Kim, D.; Ghosh, S.; Akter, N.; Kraetz, A.; Duan, X.; Gwak, G.; Rangnekar, N.; Johnson, J. R.; Narasimharao, K.; Malik, M. A.; Al-Thabaiti, S.; McCool, B.; Boscoboinik, J. A.; Mkhoyan, K. A.; Tsapatsis, M. Twin-free, directly synthesized MFI nanosheets with improved thickness uniformity and their use in membrane fabrication. *Sci. Adv.* **2022**, *8*, eabm8162.

(5) Li, Z. Y.; Li, J.; Rong, H. Z.; Zuo, J. Y.; Yang, X.; Xing, Y.; Liu, Y. S.; Zhu, G. S.; Zou, X. Q. SO_2/NO_2 Separation Driven by NO_2 Dimerization on SSZ-13 Zeolite Membrane. *J. Am. Chem. Soc.* **2022**, *144*, 6687−6691.

(6) Lai, Z. P.; Tsapatsis, M.; Nicolich, J. R. Siliceous ZSM-5 membranes by secondary growth of *b*-oriented seed layers. *Adv. Funct. Mater.* **2004**, *14*, 716−729.

(7) Lu, X. F.; Wang, H. S.; Yang, Y. W.; Wang, Z. B. Microstructural manipulation of MFI-type zeolite films/membranes: Current status and perspectives. *J. Membr. Sci.* **2022**, *662*, 120931.

(8) Jeon, M. Y.; Kim, D.; Kumar, P.; Lee, P. S.; Rangnekar, N.; Bai, P.; Shete, M.; Elyassi, B.; Lee, H. S.; Narasimharao, K.; Basahel, S. N.; Al-Thabaiti, S.; Xu, W. Q.; Cho, H. J.; Fetisov, E. O.; Thyagarajan, R.; DeJaco, R. F.; Fan, W.; Mkhoyan, K. A.; Siepmann, J. I.; Tsapatsis, M. Ultra-selective high-flux membranes from directly synthesized zeolite nanosheets. *Nature* **2017**, *543*, 690−694.

(9) Varoon, K.; Zhang, X. Y.; Elyassi, B.; Brewer, D. D.; Gettel, M.; Kumar, S.; Lee, J. A.; Maheshwari, S.; Mittal, A.; Sung, C. Y.; Cococcioni, M.; Francis, L. F.; McCormick, A. V.; Mkhoyan, K. A.; Tsapatsis, M. Dispersible exfoliated zeolite nanosheets and their application as a selective membrane. *Science* **2011**, *334*, 72−75.

(10) Lai, Z. P.; Bonilla, G.; Diaz, I.; Nery, J. G.; Sujaoti, K.; Amat, M. A.; Kokkoli, E.; Terasaki, O.; Thompson, R. W.; Tsapatsis, M.; Vlachos, D. G. Microstructural optimization of a zeolite membrane for organic vapor separation. *Science* **2003**, *300*, 456−460.

(11) Agrawal, K. V.; Topuz, B.; Pham, T. C.; Nguyen, T. H.; Sauer, N.; Rangnekar, N.; Zhang, H.; Narasimharao, K.; Basahel, S. N.; Francis, L. F.; Macosko, C. W.; Al-Thabaiti, S.; Tsapatsis, M.; Yoon, K. B. Oriented MFI Membranes by Gel-Less Secondary Growth of Sub-100 nm MFI-Nanosheet Seed Layers. *Adv. Mater.* **2015**, *27*, 3243−3249.

(12) Kim, D.; Jeon, M. Y.; Stottrup, B. L.; Tsapatsis, M. Para-Xylene Ultra-selective Zeolite MFI Membranes Fabricated from Nanosheet

Monolayers at the Air-Water Interface. *Angew. Chem., Int. Ed.* **2018**, *57*, 480−485.
(13) Qiu, H. E.; Xu, N.; Kong, L.; Zhang, Y.; Kong, X.; Wang, M. Q.; Tang, X. X.; Meng, D. N.; Zhang, Y. F. Fast synthesis of thin Silicalite-1 zeolite membranes at low temperature. *J. Membr. Sci.* **2020**, *611*, 118361.
(14) Liu, Y.; Lu, J. M.; Liu, Y. Single-Mode Microwave Heating-Induced Concurrent Out-of-Plane Twin Growth Suppression and In-Plane Epitaxial Growth Promotion of *b*-Oriented MFI Film under Mild Reaction Conditions. *Chem. Asian J.* **2020**, *15*, 1277−1280.
(15) Zhang, X.; Tong, D.; Jia, W.; Tang, D.; Li, X.; Yang, R. Studies on room-temperature synthesis of zeolite NaA. *Mater. Res. Bull.* **2014**, *52*, 96−102.
(16) Yu, L.; Grahn, M.; Hedlund, J. Ultra-thin MFI membranes for removal of C_{3+} hydrocarbons from methane. *J. Membr. Sci.* **2018**, *551*, 254−260.
(17) Liu, Y.; Qiang, W. L.; Ji, T. T.; Zhang, M.; Li, M. R.; Lu, J. M.; Liu, Y. Uniform hierarchical MFI nanosheets prepared via anisotropic etching for solution-based sub−100-nm-thick oriented MFI layer fabrication. *Sci. Adv.* **2020**, *6*, eaay5993.
(18) Liu, Y.; Li, M.; Chen, Z.; Cui, Y.; Lu, J.; Liu, Y. Hierarchy Control of MFI Zeolite Membrane towards Superior Butane Isomer Separation Performance. *Angew. Chem., Int. Ed.* **2021**, *60*, 7659−7663.
(19) Zhou, H.; Mouzon, J.; Farzaneh, A.; Antzutkin, O. N.; Grahn, M.; Hedlund, J. Colloidal Defect-Free Silicalite-1 Single Crystals: Preparation, Structure Characterization, Adsorption, and Separation Properties for Alcohol/Water Mixtures. *Langmuir* **2015**, *31*, 8488−8494.
(20) Si, D.; Zhu, M.; Sun, X.; Xue, M.; Li, Y.; Wu, T.; Gui, T.; Kumakiri, I.; Chen, X.; Kita, H. Formation process and pervaporation of high aluminum ZSM-5 zeolite membrane with fluoride-containing and organic template-free gel. *Sep. Purif. Technol.* **2021**, *257*, 117963.
(21) Fyfe, C. A.; Brouwer, D. H.; Lewis, A. R.; Chézeau, J.-M. Location of the Fluoride Ion in Tetrapropylammonium Fluoride Silicalite-1 Determined by $^{1}H/^{19}F/^{29}Si$ Triple Resonance CP, REDOR, and TEDOR NMR Experiments. *J. Am. Chem. Soc.* **2001**, *123*, 6882−6891.
(22) Mostowicz, R.; Crea, F.; B-Nagy, J. Crystallization of silicalite-1 in the presence of fluoride ions. *Zeolites* **1993**, *13*, 678−684.
(23) Attfield, M. P.; Catlow, C. R. A.; Sokol, A. A. True structure of trigonal bipyramidal SiO_4F^- species in siliceous zeolites. *Chem. Mater.* **2001**, *13*, 4708−4713.
(24) Dai, W. J.; Kouvatas, C.; Tai, W. S.; Wu, G. J.; Guan, N. J.; Li, L. D.; Valtchev, V. Platelike MFI Crystals with Controlled Crystal Faces Aspect Ratio. *J. Am. Chem. Soc.* **2021**, *143*, 1993−2004.
(25) Zhou, Y. W.; Wang, Y. C.; Ban, Y. J.; Guo, A.; Yang, K.; Cao, N.; Yang, W. S. Carbon molecular sieving membranes for butane isomer separation. *AlChE J.* **2019**, *65*, e16749.
(26) Min, B.; Yang, S.; Korde, A.; Jones, C. W.; Nair, S. Single-Step Scalable Fabrication of Zeolite MFI Hollow Fiber Membranes for Hydrocarbon Separations. *Adv. Mater. Interfaces* **2020**, *7*, 2000926.
(27) Sun, K.; Liu, B.; Zhong, S. L.; Wu, A. M.; Wang, B.; Zhou, R. F.; Kita, H. Fast preparation of oriented silicalite-1 membranes by microwave heating for butane isomer separation. *Sep. Purif. Technol.* **2019**, *219*, 90−99.
(28) Wang, Q.; Wu, A. M.; Zhong, S. L.; Wang, B.; Zhou, R. F. Highly (*h0h*)-oriented silicalite-1 membranes for butane isomer separation. *J. Membr. Sci.* **2017**, *540*, 50−59.
(29) Wu, A. M.; Tang, C. Y.; Zhong, S. L.; Wang, B.; Zhou, J. J.; Zhou, R. F. Synthesis optimization of (*h0h*)-oriented silicalite-1 membranes for butane isomer separation. *Sep. Purif. Technol.* **2019**, *214*, 51−60.
(30) Bernal, M. P.; Xomeritakis, G.; Tsapatsis, M. Tubular MFI zeolite membranes made by secondary (seeded) growth. *Catal. Today* **2001**, *67*, 101−107.
(31) Pham, T. C. T.; Kim, H. S.; Yoon, K. B. Growth of Uniformly Oriented Silica MFI and BEA Zeolite Films on Substrates. *Science* **2011**, *334*, 1533−1538.
(32) Min, B.; Yang, S. W.; Korde, A.; Kwon, Y. H.; Jones, C. W.; Nair, S. Continuous Zeolite MFI Membranes Fabricated from 2D MFI Nanosheets on Ceramic Hollow Fibers. *Angew. Chem., Int. Ed.* **2019**, *58*, 8201−8205.
(33) Lu, X. F.; Peng, Y.; Wang, Z. B.; Yan, Y. S. Rapid fabrication of highly *b*-oriented zeolite MFI thin films using ammonium salts as crystallization-mediating agents. *Chem. Commun.* **2015**, *51*, 11076−11079.
(34) Liu, Y.; Li, Y. S.; Yang, W. S. Fabrication of highly *b*-oriented MFI film with molecular sieving properties by controlled in-plane secondary growth. *J. Am. Chem. Soc.* **2010**, *132*, 1768−1769.
(35) Kim, D.; Shete, M.; Tsapatsis, M. Large-Grain, Oriented, and Thin Zeolite MFI Films from Directly Synthesized Nanosheet Coatings. *Chem. Mater.* **2018**, *30*, 3545−3551.

https://doi.org/10.1021/jacs.3c00009
J. Am. Chem. Soc. 2023, 145, 7718−7723